DOI: 10.1002/eji.201445021 Eur. J. Immunol. 2015. 45: 1680–1695

European Journal of Immunology

Human metapneumovirus infection activates the TSLP pathway that drives excessive pulmonary inflammation and viral replication in mice

Margarita K. Lay[*1], Pablo F. Céspedes*[*1], Christian E. Palavecino[1], Miguel A. León[1], Rodrigo A. Díaz[1], Francisco J. Salazar[1], Gonzalo P. Méndez[2], Susan M. Bueno[1,3] and Alexis M. Kalergis[1,3,4]*

[1] Departamento de Genética Molecular y Microbiología, Facultad de Ciencias Biológicas, Millennium Institute on Immunology and Immunotherapy, Pontificia Universidad Católica de Chile, Santiago, Chile
[2] Departamento de Anatomía Patológica, Facultad de Medicina, Pontificia Universidad Católica de Chile, Santiago, Chile
[3] INSERM U1064, Nantes, France
[4] Departamento de Reumatología, Facultad de Medicina, Pontificia Universidad Católica de Chile, Santiago, Chile

Human metapneumovirus (hMPV) is a leading cause of acute respiratory tract infections in children and the elderly. The mechanism by which this virus triggers an inflammatory response still remains unknown. Here, we evaluated whether the thymic stromal lymphopoietin (TSLP) pathway contributes to lung inflammation upon hMPV infection. We found that hMPV infection promotes TSLP expression both in human airway epithelial cells and in the mouse lung. hMPV infection induced lung infiltration of OX40L$^+$CD11b$^+$ DCs. Mice lacking the TSLP receptor deficient mice (*tslpr*$^{-/-}$) showed reduced lung inflammation and hMPV replication. These mice displayed a decreased number of neutrophils as well a reduction in levels of thymus and activation-regulated chemokine/CCL17, IL-5, IL-13, and TNF-α in the airways upon hMPV infection. Furthermore, a higher frequency of CD4$^+$ and CD8$^+$ T cells was found in *tslpr*$^{-/-}$ mice compared to WT mice, which could contribute to controlling viral spread. Depletion of neutrophils in WT and *tslpr*$^{-/-}$ mice decreased inflammation and hMPV replication. Remarkably, blockage of TSLP or OX40L with specific Abs reduced lung inflammation and viral replication following hMPV challenge in mice. Altogether, these results suggest that activation of the TSLP pathway is pivotal in the development of pulmonary pathology and pulmonary hMPV replication.

Keywords: Dendritic cells · hMPV · Inflammation · Neutrophils · OX40L · TSLP · Viral replication

Additional supporting information may be found in the online version of this article at the publisher's web-site

Correspondence: Dr. Alexis M. Kalergis
e-mail: akalergis@bio.puc.cl

*These authors contributed equally to this work.

Introduction

Human metapneumovirus (hMPV) is an enveloped virus that belongs to the *Paramyxoviridae* family, *Pneumovirinae* subfamily, and the *Metapneumovirus* genus. The hMPV genome consists of a 13.3-kb single-stranded, negative-sense RNA encoding eight messenger RNAs, which are transcribed directly from the viral genome and translated into nine different polypeptides [1, 2]. hMPV was described for the first time in 2001 as a pathogen responsible for acute respiratory tract infections in children [3]. Today, hMPV is considered the second most relevant etiological agent of acute upper and lower respiratory tract infections in children, the elderly, and immunocompromised adults [4]. Furthermore, in young children, hMPV is the second most reported cause of bronchiolitis and pneumonia after human respiratory syncytial virus (hRSV), accounting for ~10% of pediatric hospitalizations related to acute respiratory tract infection [5–7]. In addition, hMPV is the cause of outbreaks of acute respiratory tract infections with more than 10% mortality in elderly patients [8, 9]. Currently, neither safe-effective vaccines nor specific antiviral therapies are available for hMPV, although promising candidate vaccines have recently been developed [10–12].

hMPV infects preferentially airway epithelial cells (AECs) [13] and rapidly induces disruption of the architecture of the lung with an increased myofibroblast thickening adjacent to the airway epithelium. Infection proceeds with sloughing of epithelial cells, loss of cell ciliation, and acute pulmonary inflammation, which is characterized by abundant perivascular cell infiltrate, moderate peribronchiolar and bronchiolar cell infiltrates, alveolitis, and production of mucus [14–16, 38, 39]. In addition, using the BALB/c mouse model, hMPV infection was shown to induce long-term histopathologic inflammation and residual airway hyperresponsiveness [14]. Moreover, hMPV infection has previously been reported to induce a strong innate response in the airways of BALB/c mice, including robust infiltration of neutrophils and lymphocytes, as well as high levels of the inflammatory cytokines IL-6, TNF-α, and of the C-C chemokine CCL2 [17]. However, the exact mechanism that cause lung inflammation and damage by hMPV infection remains poorly characterized. It is also known that hMPV infection in BALB/c mice leads to a mixed TH response characterized by an early predominant TH1-like response with expression of IL-2, TNF-α, and IFN-γ-producing T cells, followed by a delayed TH2 response driven by IL-10-producing T cells [13]. Both, IFN-γ-secreting $CD4^+$T and $CD8^+$T cells are required for viral clearance [18, 19]. However, detectable levels of other cytokines, such as IL-4 and IL-5, are also observed at earlier times upon hMPV infection, which are thought to contribute to the development of a T_H2 immune response [20, 21].

The thymic stromal lymphopoietin (TSLP) is an epithelial cell-derived IL-7-like cytokine that contributes to mucosal immunity induced by microbes [22, 23]. Several reports suggest that TSLP is a cytokine that promotes inflammatory responses of both type 1 (T_H1) and type 2 (allergic-T_H2) profiles [24–30]. TSLP activates myeloid dendritic cells (DCs), which in turn produce chemokines including eotaxin-2, IL-8, and CCL17 (thymus and activation-regulated chemokine, TARC) that recruit eosinophils, neutrophils, and T_H2 cells, respectively [22], and the upregulation of OX40 ligand (OX40L) [31] that, as a downstream effector of the TSLP pathway, skews the differentiation of naïve $CD4^+$ T cells into both T_H1/T_H2 cells in allergic inflammation [25, 29, 30, 32]. Recently, compelling pieces of evidence suggest that the TSLP pathway plays an instrumental role in the pathogenesis of hRSV, a related paramyxovirus that displays striking similarities with hMPV in terms of disease presentation and pulmonary hyperresponsiveness. For instance, it was described that hRSV induces the production of TSLP by infected rat tracheal epithelial cells, promoting the expression of OX40L as well as the secretion of TARC/CCL17 by TSLP-stimulated DCs [33]. Furthermore, in response to hRSV, human AECs and mouse lung secrete TSLP and the blockade of TSLP signaling prevents airway hyperresponsiveness and lung immunopathology in adult mice [34]. Moreover, the blockade of TSLP and OX40L in mouse neonates before and during primary hRSV infection, respectively, prevented the enhancement of airway inflammation after reinfection [35]. Therefore, given the major role of TSLP in the pathogenesis of hRSV, in this work we sought to evaluate whether a similar pathway may be responsible for the induction of pulmonary inflammation and damage following infection with hMPV. We found that hMPV induces human AECs to produce TSLP and IL-33. Furthermore, we also observed that TSLP and TARC/CCL17 are induced in lungs of hMPV-infected mice, which had a significant infiltration of neutrophils and a significant expression of OX40L on lung $CD11b^+$DCs. Moreover, BALB/c mice lacking a functional TSLP receptor mice (*tslpr*$^{-/-}$) showed reduced inflammatory damage and viral replication in lungs, as well as a concomitant reduction in the mRNA levels of TARC/CCL17, IL-5, IL-13, and TNF-α. Consistent with the reduction of these pro-inflammatory cytokines, we observed a significant decrease in the number of neutrophils. Interestingly, comparison of cell subsets in lungs of WT and *tslpr*$^{-/-}$ mice, identified global changes in the numbers of other immune cells, such as an increase in $OX40L^+$ alveolar macrophages and in T cells in lungs of *tslpr*$^{-/-}$ mice, which are accompanied with a reduced viral load at day 4 postinfection (pi). Furthermore, the treatment of WT mice with TSLP or OX40L Abs significantly ameliorated lung inflammation and viral replication upon hMPV infection. Altogether these results suggest that the TSLP pathway is critical for hMPV immunopathogenesis.

Finally, we observed that specific depletion of neutrophils with an anti-Ly6G mAb significantly reduced lung inflammation and viral load in the lungs of hMPV-infected mice. These findings suggest that neutrophils are important mediators of the pulmonary immunopathology and key factors in controlling viral replication.

Results

hMPV infection induces expression of TSLP, IL-33, and IL-8 in human AECs

To determine whether hMPV infection induces the expression of TSLP in human AECs, human alveolar epithelial cells (A549 cells)

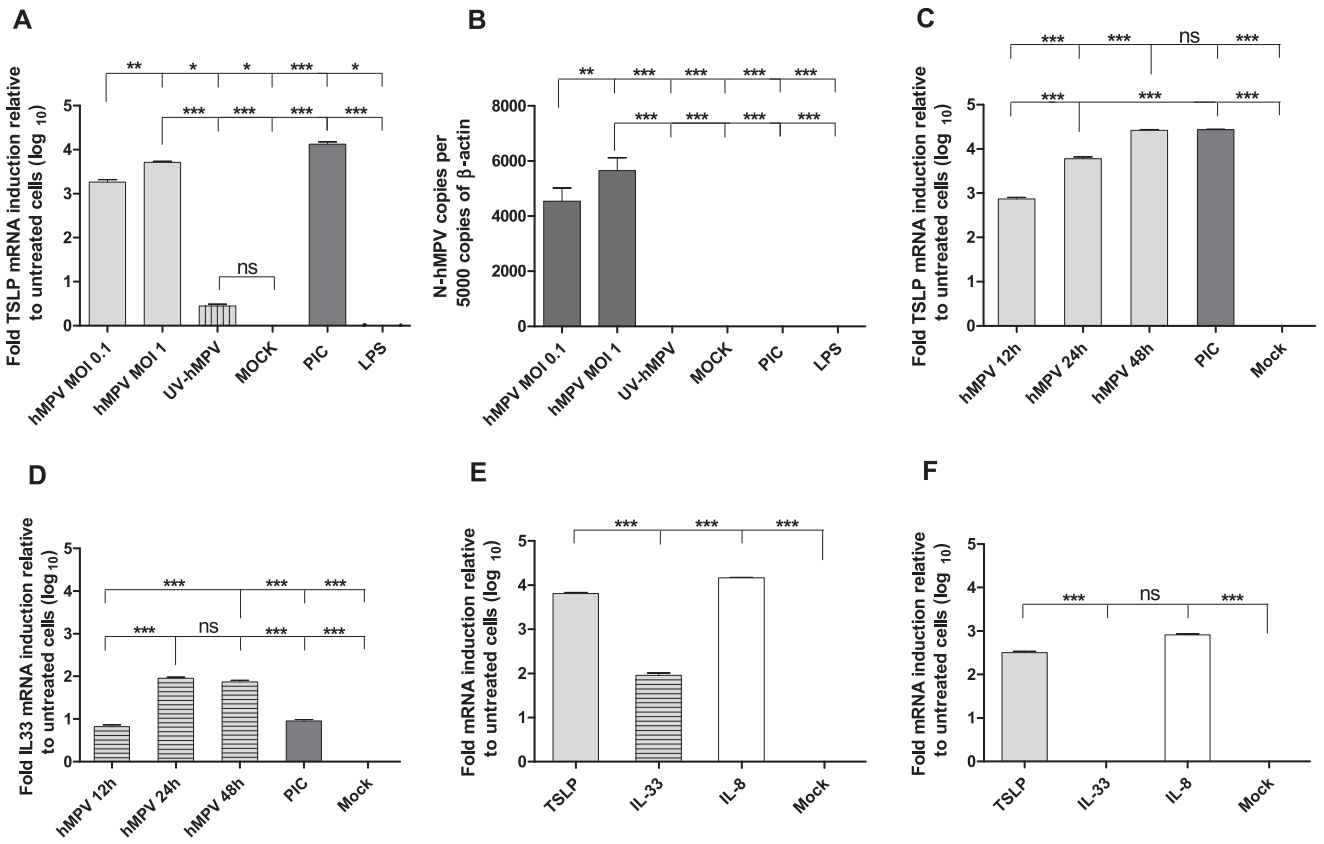

Figure 1. HMPV-infected human alveolar epithelial cells (A549 cells) induce TSLP and IL-33 gene expression. (A, B) Total RNA from A549 cells exposed to mock treatment, or UV-inactivated hMPV, or hMPV at a MOI 0.1, or hMPV at a MOI 1 was analyzed by qRT-PCR, using primers specific for (A) TSLP and (B) N-hMPV transcripts, after 24 h. (C, D) In addition, similar samples were analyzed after 12, 24, and 48 h for induction of (C) TSLP and (D) IL-33 mRNAs. Ten micrograms of polyI:C was included as a control. (E, F) Total RNA from A549 cells exposed to mock treatment, or (E) hMPV, or (F) hRSV at a MOI equal to 1 for each virus, was analyzed by qRT-PCR, using primers specific to TSLP, IL-33, and IL-8 after 24 h. Each well contained 2×10^5 cells. The data plotted represent the means ± SD of triplicate wells from a single experiment representative of three performed. Asterisk(s) means significant, $^*p < 0.05$, $^{**}p < 0.01$, $^{***}p < 0.001$; ns: not significant, one-way ANOVA test.

were exposed to mock, UV-inactivated hMPV, or hMPV at multiplicities of infection (MOIs) equal to 0.1 or 1 for 24 h. As controls for TSLP induction, the synthetic analog of double-stranded RNA polyI:C and bacterial LPS were included.

TSLP expression was determined for A549 human cells from total RNA by quantitative reverse transcriptase PCR (qRT-PCR). As shown in Figure 1A, compared to uninfected (Mock) cells, A549 cells infected with two different MOIs of hMPV significantly increased TSLP expression. These levels were comparable to 10 μg polyI:C- treated cells, which is known to produce TSLP upon intracellular binding of TLR-3 [36]. In contrast, no significant TSLP induction was observed in cells exposed to either UV-inactivated hMPV or 10 μg of LPS, which is recognized by TLR-4 expressed on the surface of cells (Fig. 1A). In addition, hMPV-infected A549 cells showed high numbers of copies of RNA encoding the hMPV nucleoprotein (N) (indicative of viral load), at both MOIs tested, after 24 h postinfection (pi) (Fig. 1B). As expected, no hMPV N RNA levels were detected in uninfected controls. These results suggest that hMPV replication is required to induce the expression of TSLP in human AECs. In addition, increased levels of TSLP mRNA were consistently observed at 12, 24, and 48 h pi (Fig. 1C).

We also evaluated whether IL-33, another epithelium-derived cytokine inducing OX40L expression on DCs [37, 38] and IL-8 (used as a control cytokine) were upregulated upon infection with hMPV. As shown in Figure 1D, a significant upregulation of the IL-33 mRNA was observed in A549 cells infected with hMPV, at 24 and 48 h pi (~2 logs) (Fig. 1D). In addition, no significant IL-33 induction was observed in cells exposed to UV-inactivated hMPV or 10 μg LPS (data not shown). When we evaluated the expression of these two AEC-derived cytokines in hMPV-infected A549 cells compared to hRSV-infected cells (at a MOI of 1), hMPV induced high levels of TSLP, comparable to IL-8, as well as significant levels of IL-33 transcripts (Fig. 1E). In contrast, A549 cells in response to hRSV produced TSLP and IL-8, but not IL-33 (Fig. 1F). These data suggest that induction of TSLP and IL-33 occurs early during the viral infection cycle due to the activation of molecules sensing viral replication in the cytosol of AECs. Also, our data suggest that TSLP and IL-33 in synergy with IL-8 may play

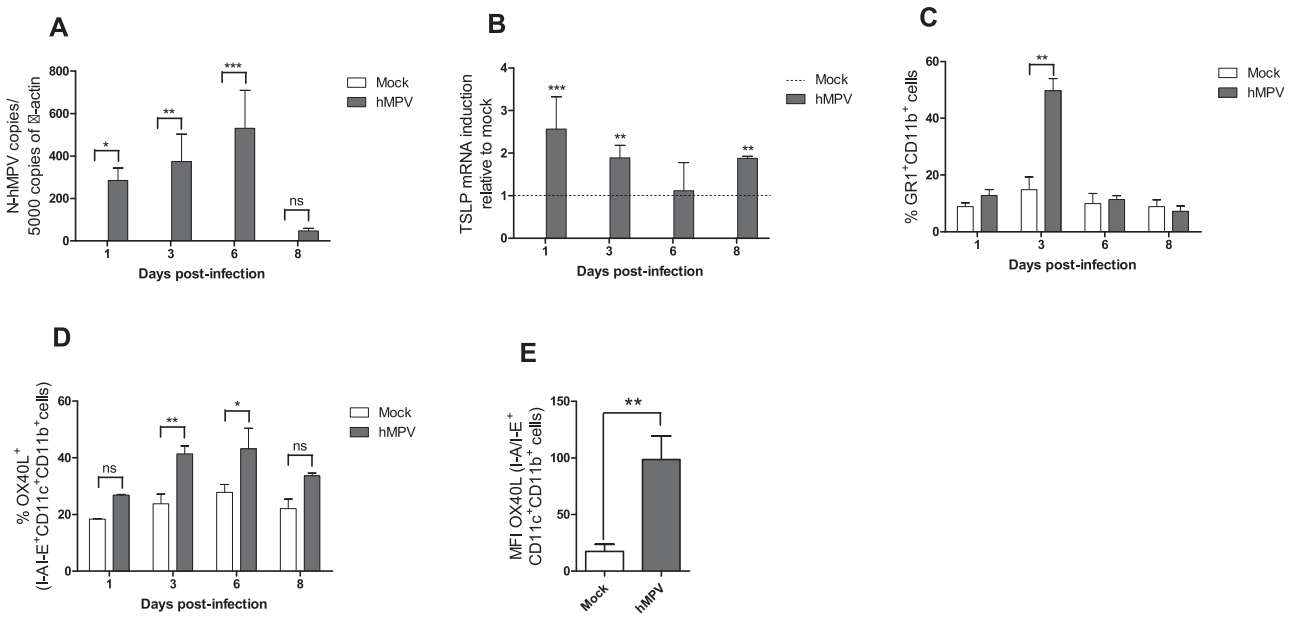

Figure 2. hMPV induces lung infiltration of OX40L$^+$/I-A/I-E^{high} CD11c$^+$ CD11b$^+$cells. (A, B) Groups of BALB/cJ mice were i.n. inoculated with hMPV or mock. At days 1, 3, 6, and 8 after inoculation, quantification of (A) viral RNA (N-hMPV) and (B) TSLP mRNA was performed at the indicated days by qRT-PCR, in lungs of mock- and hMPV-inoculated mice. (C, D) BALF or a section of a lung was collected from each mock- and hMPV-infected mice and the percentages of (C) neutrophils (Gr1$^+$/CD11b$^+$) in BALF and (D) OX40L$^+$ DCs (OX40L$^+$/I-A/I-E^{high} CD11c$^+$ CD11b$^+$), recruited to the lungs, were analyzed by flow cytometry. (E) MFI of OX40L on I-A/I-E^{high} CD11c$^+$ CD11b$^+$ DCs was also determined in lungs of hMPV-infected mice compared to uninfected animals 6 days postinfection. Data are shown as mean ± SEM of two experiments, each performed with three to four mice per group. $^*p < 0.05$; $^{**}p < 0.01$, $^{***}p < 0.001$; by two-way ANOVA (A–D) and Student's *t*-test (E).

a role in promoting lung inflammation during hMPV infection in humans.

hMPV induces TSLP expression in the mouse lung and OX40L expression on lung CD11b$^+$ DCs

To determine whether the TSLP pathway is mediating the immunopathology affecting lungs upon infection with hMPV, we evaluated the TSLP expression in lungs of mice, as well as the expression of OX40L on lung CD11c$^+$CD11b$^+$ cells. The latter cell subset, which also was positive for class II MHC, was previously described as a relevant lung DC population expressing OX40L in response to hRSV-induced TSLP [35]. This lung DC subset has also been previously defined as CD11b$^+$DCs [39]. Mice were inoculated via intranasal (i.n.) with hMPV or noninfectious LLC-MK2 cell supernatant (mock). Total RNA from lung homogenates was obtained from both experimental groups euthanized at 1, 3, 6, and 8 days pi (dpi), and quantification of viral RNA was measured from each day. Increased viral replication in lungs of hMPV-infected mice was observed at 1, 3, and 6 dpi (Fig. 2A). Likewise, a significant increase in TSLP expression was observed in lungs of both infected groups, as compared to mock controls at 1, 3, and 8 dpi (Fig. 2B), indicating that hMPV induces TSLP expression in the mouse lung. In addition, the recruitment of PMN cells (Gr-1$^+$CD11b$^+$) in bronchoalveolar lavage fluid (BALF) was significantly increased at day 3 compared to it observed in control mice, using the gating strategy described in Supporting Information Figure 1 (Fig. 2C), correlating with the increase in TSLP, at earlier times. Besides, single-cell suspensions from lung homogenates were prepared from both experimental groups at the indicated time points. On each day, the frequency of lung CD11b$^+$DCs expressing OX40L was determined by flow cytometry, using the gating strategy described in Supporting Information Figures 2 and 5. Notably, a significant increase in the percentage of OX40L$^+$CD11b$^+$ DCs was observed at days 3 and 6 in lungs of hMPV-infected mice (Fig. 2D). Moreover, after reaching a peak of frequency of these cells at day 6, returned to basal levels at day 8 pi. Furthermore, the elevated frequency of OX40L$^+$CD11b$^+$ DCs was consistent with a significant increase in the expression of OX40L (MFI, Supporting Information Fig. 2) on lung CD11b$^+$DCs from hMPV-infected mice as compared to it observed in cells from control animals (Fig. 2E). In addition, the elevated frequency of OX40L$^+$CD11b$^+$DCs coincided with the peak levels of viral replication (Fig. 2A). These results suggest that both, the increased expression levels of TSLP and the percentage of OX40L$^+$ CD11b$^+$ DCs, concur with pulmonary inflammation and an active viral replication.

TSLP receptor deficiency prevents inflammatory damage due to hMPV infection

To determine whether the TSLP pathway contributes to hMPV-mediated immunopathology, WT and *tslpr*$^{-/-}$ BALB/cJ mice were instilled via i.n. with mock or hMPV. Daily weight loss of each experimental group was recorded until day 8. Both WT and *tslpr*$^{-/-}$ hMPV-infected mice showed a significant body weight

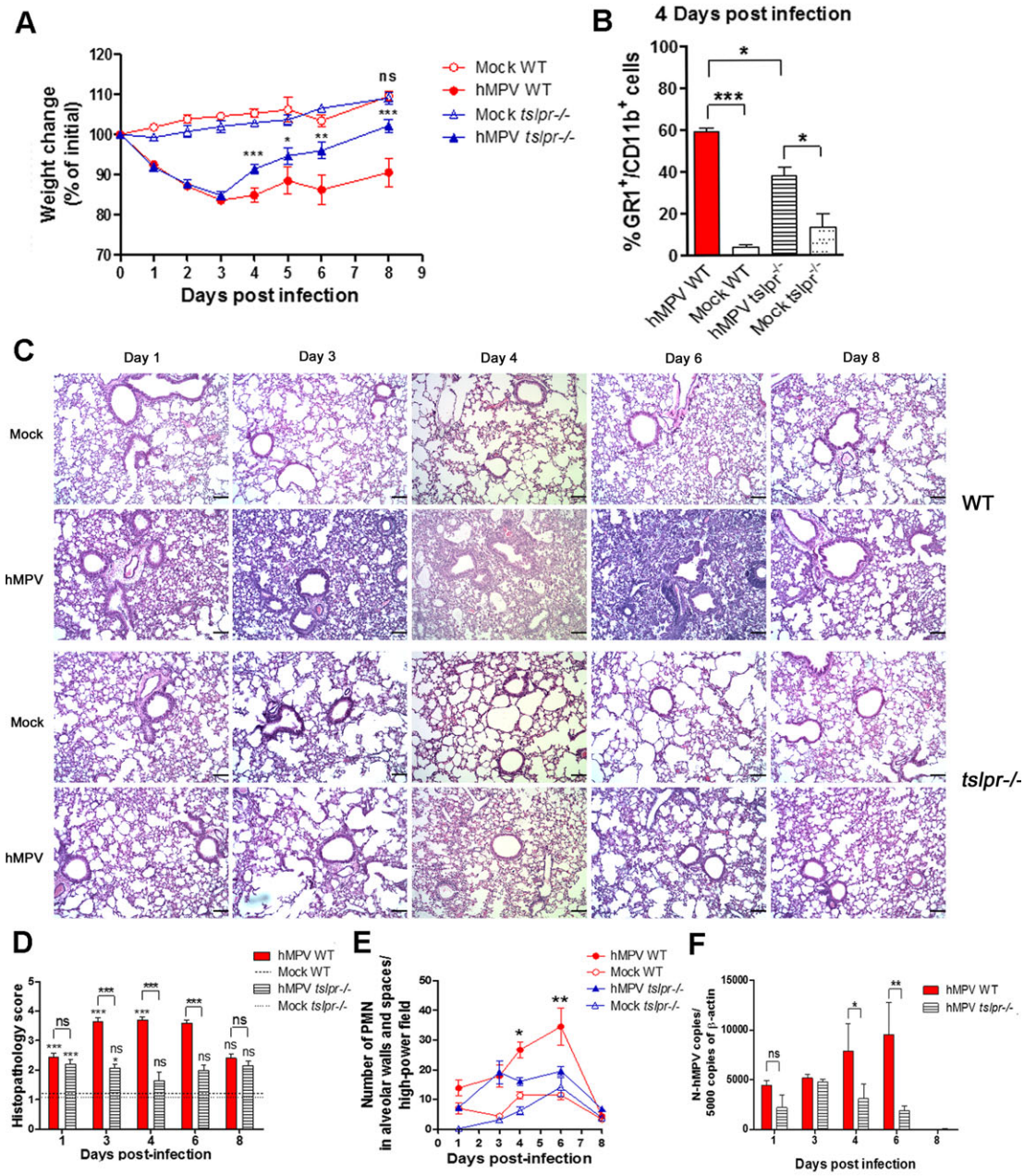

Figure 3. Lack of a functional TSLP pathway aids in recovering weight and preventing lung inflammation in hMPV-infected mice. Groups of BALB/cJ WT and TSLPR-deficient (*tslpr*$^{-/-}$) mice were i.n. inoculated with 1×10^6 PFU hMPV, or mock and daily weight loss of each experimental group was recorded until day 8. (A) Body weight is expressed as percentage of baseline weight. (B) BALF from both experimental groups after 4 dpi were collected and analyzed by flow cytometry for the percentage of PMNs ($Gr1^+/CD11b^+$) in BALF. (C) H&E staining of lung tissue from mice of each experimental group at each day. Images were acquired at 10× magnification (scale bar = 100 μm). (D) Cell infiltration in alveoli and peribronchial tissues was observed and measured by using histopathology scores. (E) The number of neutrophils in alveolar walls and spaces were also counted per high-power field and shown as mean ± SEM of five images from each animal. (F) After 1, 3, 4, 6, and 8 days postinfection, lung homogenates of WT and *tslpr*$^{-/-}$ mice of each experimental group were collected and viral RNA quantification was performed by qRT-PCR, using primers targeting the hMPV-N gene. Data are shown as mean ± SEM of three independent experiments, each performed with three or four mice per group. $p > 0.05$ = ns, $^*p < 0.05$; $^{**}p < 0.01$; $^{***}p < 0.001$; by Student's *t*-test and one-way ANOVA (B, D); or by two-way ANOVA (A, E, and F).

loss from day 1 to 3 pi (Fig. 3A). However, a significant recovery in the body weight of *tslpr*$^{-/-}$ mice was observed at day 4 pi, compared to it of WT mice (Fig. 3A). Furthermore, by day 8, while WT mice still showed significant weight loss due to hMPV infection, their *tslpr*$^{-/-}$ counterparts recovered their initial weight (Fig. 3A). Besides we found a significant lower recruitment of PMN cells in BALF from *tslpr*$^{-/-}$ mice compared to those found in BALF from WT mice at 4 dpi (Fig. 3B and Supporting Information Fig. 1). These data were consistent with lung histopathology analyses, in which lungs of hMPV-infected *tslpr*$^{-/-}$ mice showed an

appreciable reduction in cellular infiltration, especially at days 4 and 6 pi, in alveoli and peribronchial zones, as compared to lungs of hMPV-infected WT mice (Fig. 3C). Likewise, the histopathology scores revealed a significant reduction of lung cell infiltration in hMPV-infected *tslpr*$^{-/-}$ mice compared to those observed in lungs of WT infected mice after 3, 4, and 6 dpi (Fig. 3D). A further quantification of the inflammatory cell infiltrate, involving interstitial/intraalveolar zones, showed a significantly less number of PMNs in hMPV-infected *tslpr*$^{-/-}$ mice compared to hMPV-infected WT mice at 4 and 6 dpi (Fig. 3E). Taken together, these results suggest that the lack of a functional TSLP pathway significantly ameliorates lung inflammation and disease in hMPV-infected mice.

Finally, to determine whether the TSLP pathway contributes to hMPV replication in the respiratory tract, a section of a lung from hMPV-infected WT and *tslpr*$^{-/-}$ mice was collected from each animal euthanized on the days indicated above. Viral loads were quantified by qRT-PCR, using primers targeting the hMPV-N gene. Remarkably, we observed a significant reduction in hMPV-N RNAs in lungs of *tslpr*$^{-/-}$ infected mice compared to WT mice, specifically at days 4 and 6 pi (Fig. 3F). Interestingly, these findings suggest that mice lacking the TSLPR have a reduced susceptibility to hMPV infection in the airways or a limited viral replication.

TSLPR deficiency increases T-cell infiltration and OX40L$^+$ alveolar macrophages during hMPV infection

To further elucidate the mechanism behind the reduced lung damage and viral replication in the absence of the TSLPR, we performed a detailed analysis of innate and adaptive cell populations by flow cytometry in lungs of *tslpr*$^{-/-}$ and WT mice. Because recently Misharin and co-workers have characterized in more detail the populations of myeloid cells in the mouse lung, we therefore used similar markers and gating strategies to analyze the proportions of different lung immune cells [39]. These analyses included alveolar macrophages, lung DCs, CD8$^+$ T and CD4$^+$ T cells, among others (Fig. 4 and Supporting Information Figs. 3–5). Particularly, we found a higher number of OX40L^{high} MHC-II$^+$ alveolar macrophages in *tslpr*$^{-/-}$ mice than WT mice infected with hMPV after 4 dpi (Fig. 4A and Supporting Information Fig. 5). Because it is known that alveolar macrophages behave similarly as the anti-inflammatory M2 macrophages, these results suggest that a specific population of alveolar macrophages expressing OX40L, whose activation is independent of the TSLP pathway, could be contributing in reducing lung inflammation in hMPV-infected *tslpr*$^{-/-}$ mice. Furthermore, we did not observe significant differences in the number of either OX40L^{low}CD103$^+$ or OX40L^{neg}CD11b^{low} CD103$^+$ DCs when the frequency of these cells in lungs of WT mice was compared with those of *tslpr*$^{-/-}$ mice (Fig. 4B and C and Supporting Information Figs. 5 and 6). In addition, a significant difference was observed in the numbers of lung pDCs between hMPV-infected WT and *tslpr*$^{-/-}$ mice (Fig. 4D and Supporting Information Fig. 6). We also noticed an increase in the number of OX40L^{neg}CD11b^{low} CD103$^+$ DCs, NK cells, and B cells in both in *tslpr*$^{-/-}$ and WT mice infected with hMPV when compared to their respective mock groups, which is indicative of a consistent activation of the immune response upon infection with hMPV (Fig. 4C, E, and F and Supporting Information Figs. 5 and 6). In contrast, we observed a reduction in neutrophils in lung parenchyma of *tslpr*$^{-/-}$ mice than in those of WT mice infected with hMPV (Fig. 4G and Supporting Information Fig. 3), being consistent with the reduction of PMNs measured in the histological study mentioned above. Importantly, the observed higher significant number of pDCs in infected lungs of WT mice than in that of *tslpr*$^{-/-}$ mice suggests that the recruitment of these cells may also be contributing to inflammation in WT mice.

Furthermore, an increase in both CD4$^+$ and CD8α$^+$ T cells was observed in BALF from *tslpr*$^{-/-}$ mice compared to their respective mock group (Fig. 4H and I and Supporting Information Fig. 4). In addition, a greater number of CD4$^+$ and CD8α$^+$ T cells was observed in lungs from *tslpr*$^{-/-}$ than in WT mice infected with hMPV when compared to their respective mock groups (Fig. 4J and K and Supporting Information Fig. 4). These results suggest that a higher recruitment and activation of CD4$^+$ and CD8α$^+$ T cells in lungs of *tslpr*$^{-/-}$ mice compared to in those of WT may promote a more efficient viral clearance in these mice upon challenge with hMPV.

TSLPR deficiency decreases IL-10$^+$IL-13$^+$ T cells, CCL17, and cytokine expression after hMPV infection

In order to better characterize the immune milieu defined by the absence of the TSLPR and its influence in pulmonary pathogenesis, we evaluated the phenotype of CD4$^+$ and CD8$^+$ T cell populations by intracellular flow cytometry analysis (described in Supporting Information Fig. 4). These analyses included intracellular staining for IFN-γ, TNF-α, IL-4, IL-10 IL-12, and IL-13 in these two T-cell populations. At the fourth day pi, we found a decrease in IL-10-producing CD4$^+$ and CD8$^+$ T cells in lungs of *tslpr*$^{-/-}$ mice, which was significant for CD4$^+$ T cells (Fig. 5A and B). Similar decrease was observed in lungs of hMPV-infected *tslpr*$^{-/-}$ mice for IL-13-secreting CD4$^+$ T cells when compared to WT mice. We also found a nonsignificant reduction of IFN-γ-, TNF-α-, IL-4-, and IL-12-producing CD4$^+$ and CD8$^+$ T cells in *tslpr*$^{-/-}$ mice when compared with WT mice (Fig. 5A and B). These results suggest that at the fourth day pi, the TSLP pathway globally modulates the secretion of different T cell cytokines, yet more significantly, the secretion of the cytokines IL-10 and IL-13.

Next, we tested the gene expression of the cytokines IL-4, IL-5, IFN-γ, IL-10, and TNF-α, which are known to be upregulated during hMPV infection [13, 44, 45] and IL-13. Low levels and no significant differences in the expression of IL-4, IL-5, IL-10, IL-13, IFN-γ, and TNF-α were detected between the two hMPV-infected experimental groups at 4 dpi by qRT-PCR (Fig. 5C). In contrast, an overall increase in the expression of these citokines was observed in lungs of WT mice at 6 dpi. Augmented levels of IL-4, IFN-γ, and IL-10 were also observed in *tslpr*$^{-/-}$ mice. However, a significant reduction in IL-5, IL-13, and TNF-α levels were detected in lungs of hMPV-infected *tslpr*$^{-/-}$ mice compared to in lungs

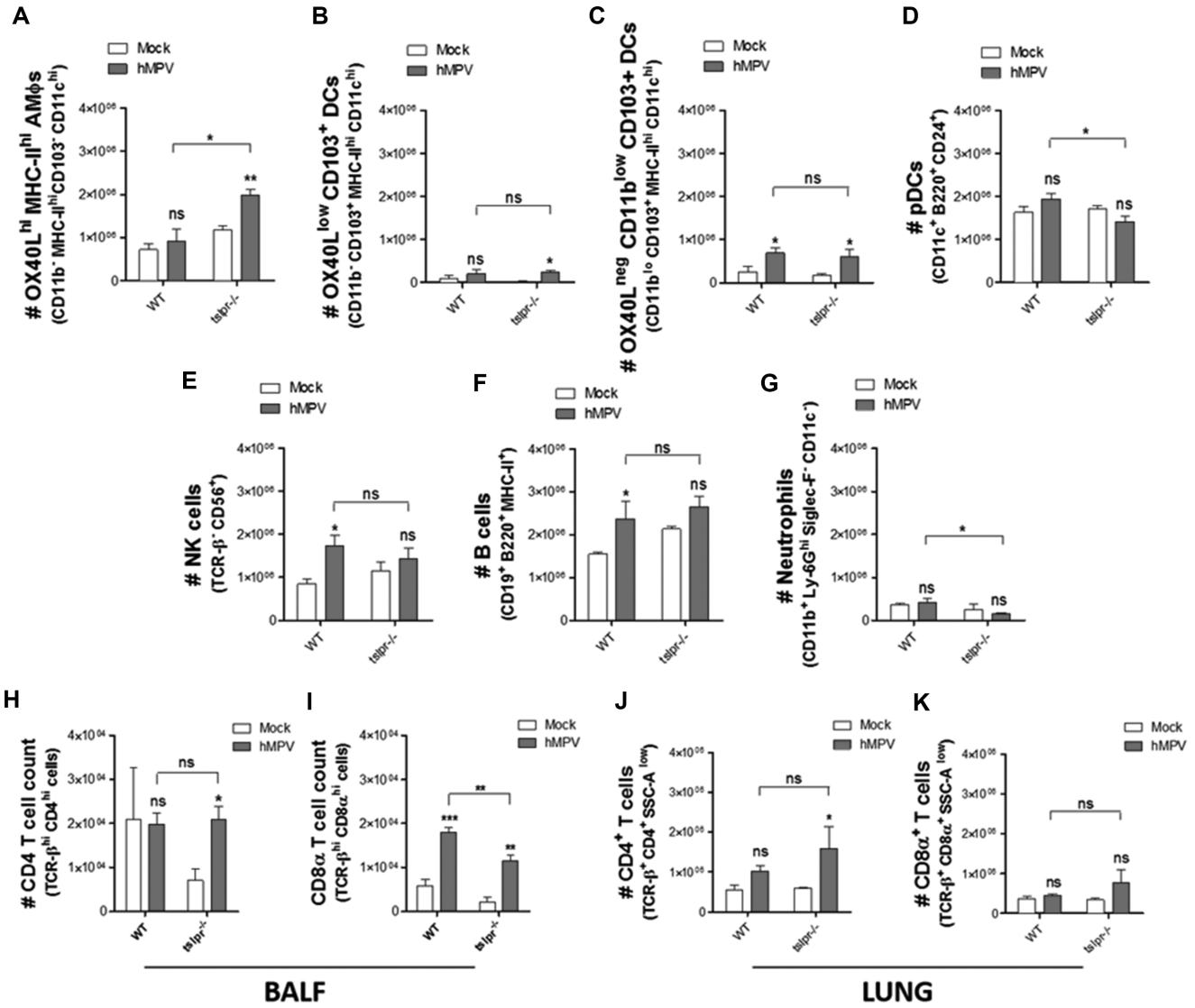

Figure 4. Lack of a functional TSLPR pathway induces an increased frequency of OX40L$^+$ alveolar macrophages, CD103$^+$ DCs and CD4$^+$ T cells in BALF and in lungs of *tslpr*$^{-/-}$ mice. Groups of BALB/cJ WT and *tslpr*$^{-/-}$ mice were i.n. inoculated with 1×10^6 PFU hMPV or mock. (A–G) Four days postinfection, lungs from both experimental groups were collected and analyzed by flow cytometry with lineage-specific markers for (A) OX40L^{hi}MHC-II^{hi} alveolar macrophages, (B) OX40L^{low}CD103$^+$ DCs, (C) OX40L^{neg}CD11b^{low}CD103$^+$ DCs, (D) CD11c^{int}B220$^+$CD24$^+$ pDCS, (E) TCR-β$^-$CD49b$^+$CD56$^+$ NK cells, (F) CD19$^+$B220$^+$MHCII$^+$ B cells, and (G) Siglec-F$^-$ CD11b$^+$Ly-6G^{hi} neutrophils. (H–K) Four days postinfection, (H, I) BALF and (J, K) lungs from both experimental groups were collected and the absolute numbers of (I, K) CD8$^+$ and (H, J) CD4$^+$ T cells were analyzed by flow cytometry. The absolute numbers of each of the indicated cell populations are shown as mean ± SEM of four mice per group from a single experiment. $p > 0.05$ = ns, $^*p < 0.05$; $^{**}p < 0.01$; Student's *t*-test.

of infected WT mice at this time point (Fig. 5D). Furthermore, these data suggest that a lack of the TSLPR in hMPV-infected mice reduces the production of several TH-secreted inflammatory mediators, including IL-5/IL-13 and TNF-α, which are T_H2- and T_H1-related cytokines, respectively. TARC/CCL17 is a known chemokine induced specifically by TSLP and IL-33-activated DCs [22, 23, 40]. Thus, to determine whether hMPV infection induces TARC/CCL17 expression in lungs of mice, via activation of the TSLP pathway, levels of this chemokine were determined by qRT-PCR in RNA from lungs of infected or mock-inoculated WT and *tslpr*$^{-/-}$ mice at various dpi (Fig. 5E). We found an increase in TARC/CCL17 expression in the airways at days 1 and 3 pi, in both WT- and *tslpr*$^{-/-}$-infected mice, relative to uninfected controls (Fig. 5E), suggesting that lung stimulated-DCs, likely by IL-33, were producing TARC/CCL17. However, at 6 dpi we observed a significant decrease in TARC/CCL17 expression in lungs of *tslpr*$^{-/-}$ compared to in those of WT-infected mice (Fig. 5E). These results indicate that the TSLPR is not necessary for the expression of TARC/CCL17 in vivo during hMPV infection at earlier times, and that an alternative receptor, such as ST2, and the IL-33 pathway may be inducing its early expression in the airways, in similar manner as previously reported [40]. Rather, TSLPR is important in the production of this chemokine at later times (6 dpi) upon hMPV infection.

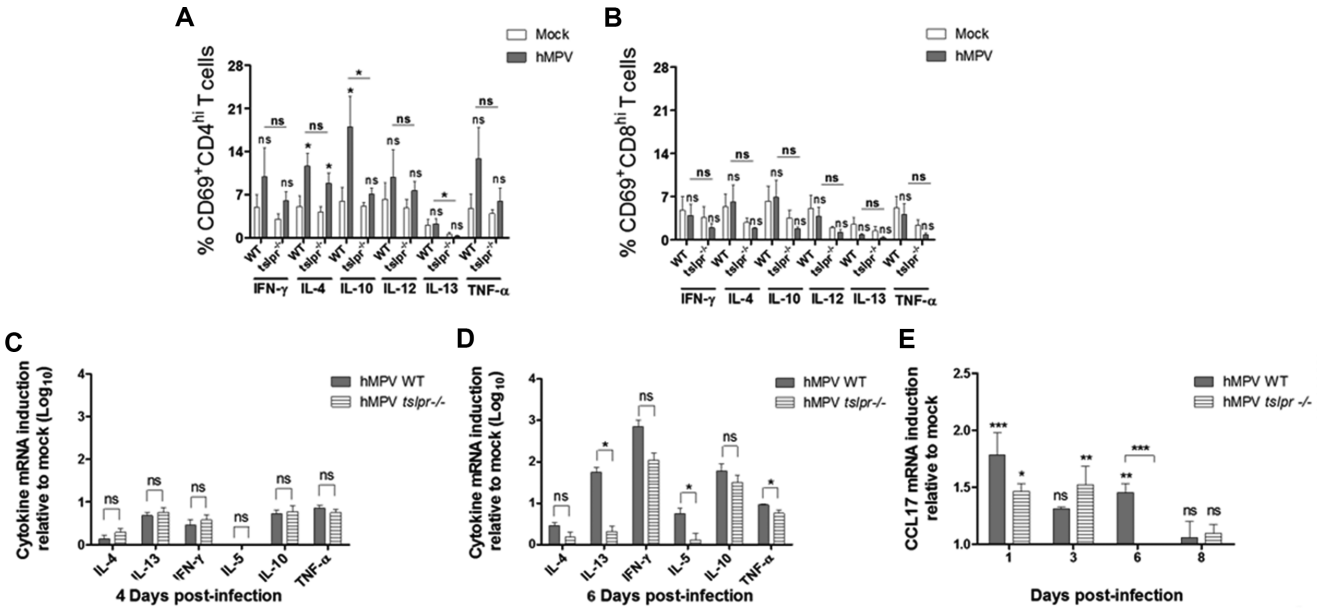

Figure 5. Deficiency of TSLPR dampens the induction of IL-10- and IL-13-producing T cells and impairs the sustained expression of IL-5, IL-13, TNF-α, and TARC/CCL17 in lungs after hMPV infection. Groups of BALB/cJ WT and *tslpr*$^{-/-}$ mice were i.n. inoculated with 1×10^6 PFU hMPV or mock, and lungs from both experimental groups after 4 days post-infection (dpi) were collected. (A, B) Specific cytokine-producing subsets within the (A) CD4$^+$ and (B) CD8$^+$ T cell compartments in lungs of mock- and hMPV-inoculated *tslpr*$^{-/-}$ and WT mice were analyzed by flow cytometry with intracellular staining for IFN-γ, TNF-α, IL-4, IL-10, IL-12, and IL-13. The percentages of cytokine-producing cells are shown as mean ± SEM of four mice per group from a single experiment. (C, D) Lung homogenates of mice, in each experimental group, were collected at (C) 4 and (D) 6 dpi and quantification of RNA was assessed by qRT-PCR, using primers targeting murine IL-4, IL-13, IFN-γ, IL-5, IL-10, and TNF-α genes. Data are shown as mean ± SEM of two experiments, each performed with four mice per group. (E) 1, 3, 6, and 8 dpi, lung homogenates of mice of each experimental group were collected and quantification of RNA was assessed by qRT-PCR, using primers targeting the TARC/CCL17 gene. Data are shown as mean ± SEM of two experiments each performed with four mice per group. Significance was calculated compared against mock-inoculated mice. $p > 0.05$ = ns, $^*p < 0.05$; $^{**}p < 0.01$, Student's *t*-test.

Treatment with neutralizing α-TSLP and α-OX40L reduces lung inflammation and hMPV replication

To further elucidate the contribution of the TSLP pathway in lung inflammation and viral replication after hMPV infection, TSLP and OX40L were blocked using neutralizing Abs before the onset of disease. At 24 h before and at the time of hMPV infection, mice were injected with 150 μg and 50 μg of α-TSLP, respectively. PBS and isotype control Ab were included in all experiments. The effect of TSLP and OX40L blockade on PMN cells recruitment in BALF (analyzed in a similar manner as in Supporting Information Fig. 1) and viral replication in lungs were determined after 3 dpi, the peak day for both parameters at that viral dose, and 6 dpi. As shown in Figure 6A, at day 3 pi, the blockade of the TSLP/OX40L pathway resulted in a significant reduction in recruitment of neutrophils in the airways, as compared to untreated hMPV-infected controls. By day 6, all animal groups had resolved the neutrophil infiltration (Fig. 6B). Notably, as for viral load measurements, a significant reduction in hMPV-N RNA levels was observed in mice receiving α-OX40L treatments, at both 3 and 6 dpi (Fig. 6C and D). However, a significant reduction in viral load was only observed at day 6 pi in mice receiving α-TSLP treatment. These results support our data obtained with mice lacking the TSLPR and suggest that blocking components of the TSLP/OX40L pathway, especially the OX40L protein, can promote a more efficient clearance of hMPV from lungs of infected mice.

Blocking the TSLP pathway reduces recruitment of OX40L$^+$ DCs into the MLNs and lung pathology

We also determined whether antibody treatments for blocking the TSLP pathway modulate the recruitment of OX40L$^+$CD11b$^+$ DCs to the MLN and lung pathology. Flow cytometry analyses were performed at day 6 pi to quantify the frequency of OX40L$^+$CD11b$^+$ DCs in MLN from hMPV-infected mice untreated and treated with α-TSLP or isotype control (Fig. 6E and Supporting Information Fig. 6). We found a significant reduction in the percentage of OX40L$^+$CD11b$^+$ DCs in the lung draining MLN of hMPV-infected mice treated with α-TSLP, as compared to infected control animals (Fig. 6E). These data suggest that TSLP blockade reduces the recruitment of OX40L expressing CD11b$^+$ DCs to the MLN after hMPV infection. In addition, we observed diminished histopathology scores in lungs of hMPV-infected mice that were treated with blocking antibodies against either TSLP or OX40L (Fig. 6F). In agreement with this notion, histopathology analyses at day 6 pi showed that blockade of either TSLP or OX40L, significantly reduced immune cell infiltration in both

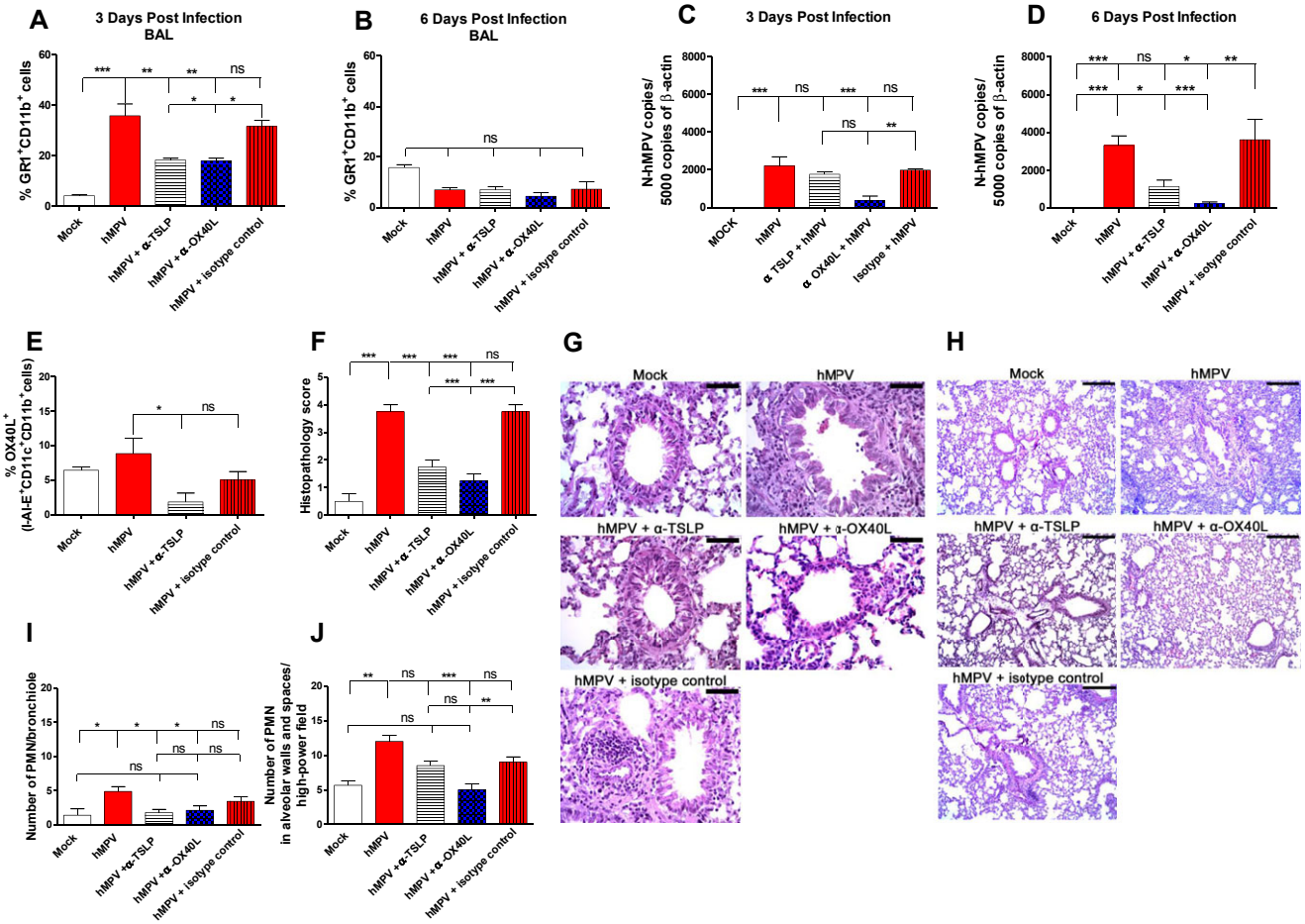

Figure 6. Treatment with α-TSLP and α-OX40L neutralizing antibodies reduces lung inflammation, hMPV replication, and the recruitment of OX40L$^+$ DCs in the MLN. Groups of BALB/cJ mice were treated with PBS, or 150 μg α-TSLP, or 150 μg α-OX40L, or 150 μg isotype control antibodies via i.p. Twenty-four hours later, mice were i.n. inoculated with 0.5×10^6 PFU hMPV or mock, and additionally treated with 50 μg of the corresponding mAbs. (A, B) The percentage of PMNs (Gr1$^+$/CD11b$^+$) in BALF from each of the experimental groups at (A) day 3 and (B) day 6 postinfection were analyzed by flow cytometry. (C, D) Lung homogenates of each experimental group were collected at (C) day 3 and (D) day 6 postinfection, and quantification of viral RNA was performed by qRT-PCR, using primers targeting the hMPV-N gene. Data are shown as mean ± SEM of two experiments, each performed with three mice per group. (E) At day 6 after inoculation, MLNs from animals of each of the experimental groups were collected and analyzed by flow cytometry for the frequency of OX40L-expressing DCs. (F) In addition, at day 6 after inoculation, a portion of a lung of mice of each group was fixed, prepared, and stained with H&E. Images obtained per sample were blind scored for histopathology. (G, H) Images were acquired at (G) 40× and (H) 10× magnification (scale bar = 50 and 200 μm, respectively). (I, J) The number of neutrophils per a bronchial section and per alveolar walls and spaces were also counted using a high power field. Data shown as mean ± SEM of five images/scores pooled from six mice from two experiments. $p > 0.05$ = ns, $^*p < 0.05$; $^{***}p < 0.001$; One-way ANOVA (A–F and I–J).

peribronchial zones (Fig. 6G) and in alveoli and lung interstitium, which suggest a reduced inflammation of lung parenchyma (Fig. 6H). Furthermore, a quantification of the amount of PMNs in the inflammatory infiltrates involving peribronchial areas (peribronchiolitis) (Fig. 6I) and interstitial/intra-alveolar zones (interstitial pneumonitis/alveolitis) (Fig. 6J) was assessed. We observed a significant decrease in PMN infiltration with the anti-OX40L treatment in both areas, but only in the peribronchial areas with the anti-TSLP treatment in lungs of hMPV-infected mice (Fig. 6I and J). Taken together, these results suggest that treatment with α-TSLP reduces infiltration of OX40L$^+$CD11b$^+$ DCs in MLN and that blocking of the TSLP/OX40L pathway with neutralizing Abs significantly ameliorates lung damage, supporting the role of TSLP and its receptor in the pulmonary immunopathology of the hMPV infection in the mouse model.

Role of neutrophils in hMPV-infected WT and *tslpr*$^{-/-}$ mice

To further elucidate the mechanism behind the reduced lung damage and viral replication in the absence of the TSLPR after hMPV inoculation in mice, we evaluated the role of the neutrophils in the pathogenesis of hMPV infection in both WT and *tslpr*$^{-/-}$ mice, using a similar approach, as previously reported for hRSV [41]. Groups of 6- to 8-week-old BALB/cJ WT and *tslpr*$^{-/-}$ mice were depleted thorough i.p. injection of anti-Ly6G or rat IgG2a

isotype control Abs. As a result, we observed a significant reduction of neutrophils in blood, BALF and lungs from both WT and *tslpr*$^{-/-}$ mice treated with anti-Ly6G, but not in those treated with the isotype control (Supporting Information Figs. 7A–E) indicating that the depletion of neutrophils worked efficiently. We first evaluated lung inflammation by performing a histopathology score and by counting the amount of neutrophils in the inflammatory infiltrates, which involves both peribronchial areas (peribronchiolitis) and interstitial/intra-alveolar zones (interstitial pneumonitis/alveolitis). We observed a significant reduction in the histopathology score of hMPV-infected WT mice, but not in hMPV-infected *tslpr*$^{-/-}$ mice, treated with the anti-Ly6G mAb when compared with those treated with the isotype control mAb (Supporting Information Fig. 8A), suggesting that neutrophil depletion in hMPV-infected WT mice reduce lung inflammation and damage. In addition, this reduction in the histopathology score was similar to that observed in hMPV-infected *tslpr*$^{-/-}$ mice either with or without neutrophil depletion. Furthermore, the number of neutrophils, in alveolar spaces and walls as well as in bronchioles, was significantly lesser in hMPV-infected *tslpr*$^{-/-}$ and WT mice treated with the anti-Ly6G mAb compared to those treated with the isotype control mAb (Supporting Information Fig. 8B and C). Moreover, a significant reduction in the number of PMN cells in alveolar spaces and walls, but not in peribrochial areas, was observed in hMPV-infected *tslpr*$^{-/-}$ mice treated with isotype control mAb compared to hMPV-infected WT mice treated with the same mAb. Taken together, these data suggest that neutrophils play a key role in lung inflammation and damage in hMPV-infected WT mice, but it is not relevant in hMPV-infected *tslpr*$^{-/-}$ mice. In addition, to further understand the reduction in viral load in *tslpr*$^{-/-}$ mice, we evaluated the role of neutrophils in viral replication in lungs of hMPV-infected WT and *tslpr*$^{-/-}$ mice. Viral load was quantified in WT and *tslpr*$^{-/-}$ mice treated with anti-Ly6G mAb or isotype control mAb after hMPV infection by qRT-PCR. Remarkably, we found a significant reduction of viral RNA copies in lungs from hMPV-infected WT mice treated with the anti-Ly6G mAb when compared with those treated with the isotype control mAb, which reached similar levels to hMPV-infected *tslpr*$^{-/-}$ mice treated with the isotype control mAb (Supporting Information Fig. 8D). Besides, we also found a greater reduction in viral load of hMPV-infected *tslpr*$^{-/-}$ mice treated with the anti-Ly6G mAb compared with hMPV-infected WT mice treated with the anti-Ly6G mAb. These results suggest that the recruitment of neutrophils in the airways, which is also dependent of the TSLP pathway, is supporting, by a still unknown mechanism, viral replication in lungs of hMPV-infected mice. Taken together, the activation of the TSLP pathway after hMPV infection in mice may contribute to the recruitment of neutrophils population within the lungs of infected animals, promoting lung inflammation, damage, and viral replication.

To further explore the participation of neutrophils in the generation of the TSLP pathway dependent-lung damage and viral replication during hMPV infection, we determined the presence of CD4$^+$ and CD8$^+$ T cells in BALF and in lungs of hMPV-infected WT and *tslpr*$^{-/-}$ mice treated with the anti-Ly6G mAb compared to those treated with the isotype control mAb. Interestingly, we observed a significant increase in the frequency of CD4$^+$ in BALF and CD4$^+$ and CD8$^+$ T cells in lungs of *tslpr*$^{-/-}$ mice, but not significant differences of those cells in WT mice, when treated with the anti-Ly6G mAb and compared to those treated with the isotype control mAb upon hMPV infection (Supporting Information Fig. 9). Moreover, no changes in recruitment of the T-cell subsets were observed in tissues from mice of the respective mock groups. These results suggest that neutrophils are controlling the recruitment and activation of T cells in *tslpr*$^{-/-}$ mice, but not in WT mice. Furthermore, the production of several cytokines produced by CD4$^+$ and CD8$^+$ T cells in lungs of mice of each of these experimental groups were assessed, as described in the material and methods section. A significant reduction in TNF-α and IL-13 production, which are known to be secreted by neutrophils in lungs [42], in CD8$^+$ T cells but not in CD4$^+$ T cells was found in hMPV-infected WT and *tslpr*$^{-/-}$ mice when treated with the anti-Ly6G mAb compared to those treated with the isotype control mAb (Supporting Information Fig. 10). The significant decrease in TNF-α levels in CD8$^+$ T cells were consistent with those observed by performing an ELISA for TNF-α detection (data not shown). These results suggest that neutrophils may modulate TNF-α and IL-13 production and/or are a source of those cytokines in response to hMPV infection, similar to what has been previously reported for hRSV [41] Furthermore, anti-Ly6G treatment strongly inhibited IL-12 and IFN-γ production in CD4$^+$/CD8$^+$T cells from both WT and *tslpr*$^{-/-}$ mice infected with hMPV (Supporting Information Fig. 10). Moreover, we observed that the anti-Ly6G treatment significantly decreased the production of IL-10 and IL-4 in both CD4$^+$ CD8$^+$ T cells from *tslpr*$^{-/-}$ mice as compared to either their isotype control mAb or WT counterpart, and decreased both cytokines produced by CD8$^+$ T cells from WT mice. These results suggest that the presence of neutrophils sustain the induction of classical T_H1 and T_H2 cytokines in both WT and *tslpr*$^{-/-}$ mice, affecting particularly the production of T_H2 type cytokines in *tslpr*$^{-/-}$ mice upon hMPV infection.

Discussion

In this study, we demonstrated for the first time that an active hMPV infection induces human AECs to produce a robust and persistent TSLP and IL-33 expression in vitro. Moreover, we also showed that hMPV induces TSLP and TARC/CCL17 in lungs of infected mice, which is a T_H2-enhancing chemokine [22]. In addition, in this report we demonstrated that hMPV infection induces CD11b$^+$ DCs to express OX40L in WT BALB/c mice, which is concomitant with a PMN infiltration and hMPV replication within the lung. Moreover, the treatment with α-TSLP Ab was sufficient to reduce the recruitment of OX40L$^+$ DCs in lung draining MLN of hMPV-infected mice, suggesting that TSLP is a pivotal molecule in inducing expression of OX40L on lung DCs. Although these results suggest that OX40L correlates with lung inflammation, data obtained with *tslpr*$^{-/-}$ mice, which displayed an increased expression of OX40L in alveolar macrophages despite having a

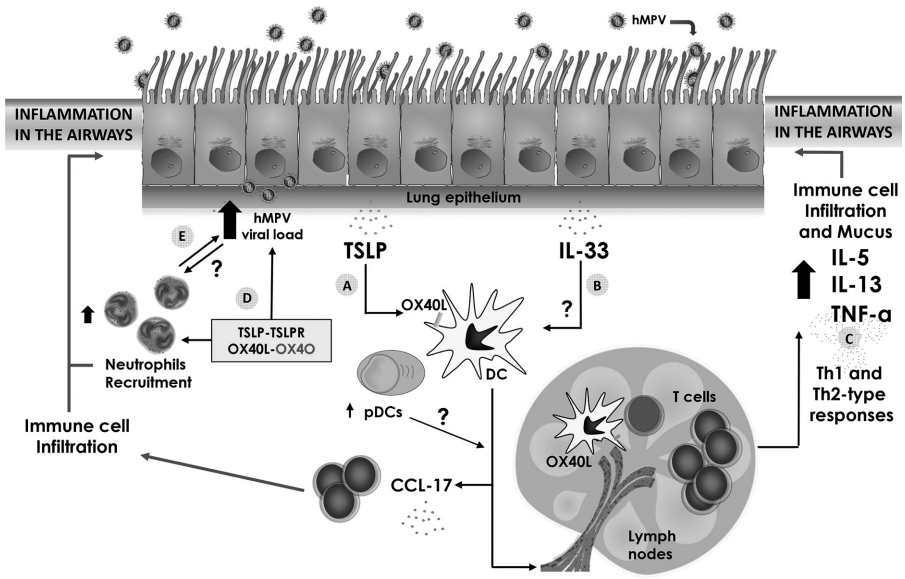

Figure 7. Proposed model for the activation of the TSLP pathway upon infection with hMPV. (A) hMPV induces AECs to secrete TSLP, which in turn induces DCs to express OX40L and secrete TARC/CCL17. In response, immune cells are attracted to the site of infection, contributing to airway inflammation. OX40L$^+$ DCs then migrate to the lung-draining MLN to prime naïve T cells. (B) hMPV induces AECs to secrete IL-33. Whether IL-33 binds to its ST2 receptor to further activate the OX40L pathway in this context, is not known. (C) After being primed by activated DCs (OX40L$^+$), naïve T cells differentiate into T_H1 and T_H2 cells, which by secreting TNF-α, IL-5, and IL-13, promote an increase in PMN cell recruitment and an induction of mucus secretion and lung inflammation after hMPV infection. (D) The activation of pathways, involving TSLP-TSLPR and OX40L-OX40(/or other ligands) interactions, may induce the recruitment of neutrophils and an increased replication of hMPV in the lung. (E) The mechanisms underlying the increased replication of hMPV, as a result of neutrophil recruitment within the airways, and the interdependence between both processes, require further studies.

nonfunctional TSLP–TSLPR axis, suggest that TSLP and inflammation are not exclusively dependent on the expression of OX40L on APCs.

In attempting to understand the mechanism behind the enhanced resolution of the pulmonary pathology observed in *tslpr*$^{-/-}$ mice, we performed flow cytometry analyses to study different immune cell populations inhabiting the mouse lung upon hMPV infection. First, we observed several changes in airway immune cells, which are summarized as follows: at the 4 day after infection with hMPV, we identified an increase in the population of OX40L^{high} alveolar macrophages in lungs of *tslpr*$^{-/-}$ mice. Since, MFI values for OX40L on these cells did not differ from those from WT mice, OX40L expression could likely be mediated by other inflammatory mediators, such as prostaglandin E_2 [43]. Importantly, OX40L^{high} alveolar macrophages may be contributing in reducing lung inflammation in hMPV-infected *tslpr*$^{-/-}$ mice, specifically by regulating neutrophil recruitment, as previously shown for alveolar macrophages in other pathological conditions [44]. In addition, this finding indicates that the expression of OX40L is not exclusive on DCs of the respiratory tract and it does not depend exclusively on TSLPR signaling. It also suggests that the effector functions of OX40L expressed on the surface of APCs may be highly dependent on the immune milieu on which it mediates downstream processes.

Secondly, we observed an increase in pDC and in NK cells in lungs of WT mice but not in those of *tslpr*$^{-/-}$ mice upon infection with hMPV, which despite lacking expression of OX40L could be contributing to lung inflammation by secreting an array of pro-inflammatory cytokines including IL-4, IL-5, and IL-13 [45]. The increased frequency of NK cells found in WT mice but not in their *tslpr*$^{-/-}$ counterparts may be due to the observed higher expression of CCL17/TARC, which is known to chemoattract NK cells [46]. This cell population may further contribute to airway inflammation by secreting IL-5 in the airways [47, 48]. Third, our data suggest that the TSLP pathway is inducing the secretion of IL-10 and IL-13 by T cells. This is in agreement with a reduction of IL-13 in *tslpr*$^{-/-}$ mice shown in a previous study with hRSV [49, 50]. Fourth, we observed elevated numbers of CD4$^+$ and CD8α$^+$ T cells in BALF and lungs from *tslpr*$^{-/-}$ mice compared to their mock groups, being dissimilar to the T-cell response observed in lungs of the WT group. This could indicate that a higher recruitment and activation of these two T-cell subsets are likely aiding in limiting viral replication more efficiently in lungs of *tslpr*$^{-/-}$ than in those of WT mice. In addition, decreasing T_H2 cytokines and maintaining IFN-γ levels, as shown in this study (Fig. 5D), could likely be favoring a more predominant T_H1 response, which could be activating more effectively CD4$^+$ and CD8$^+$ T cells to clear hMPV infection from lungs. Thus, activation of the TSLP pathway by hMPV could be a mechanism to hamper or delay a more efficient antiviral T_H1 response.

Remarkably, we also found that lack of a functional TSLP pathway significantly impairs hMPV replication in lungs of *tslpr*$^{-/-}$ mice after 4 dpi. Furthermore, WT mice treated with α-TSLP and α-OX40L Abs reduce significantly viral replication after 6 days and

as early as 3 days upon hMPV infection, respectively. Moreover, we observed a significant reduction of viral replication in mice deficient in TSLPR, which was greater in these animals with neutrophil depletion. Altogether, these findings suggest a potential role of neutrophils in hMPV spread. Three possibilities may explain this finding: (i) neutrophils could be inhibiting the efficient antiviral response to hMPV, mainly given by $CD4^+$ and $CD8^+$ T cells, via their secreted killing products (H_2O_2, arginase-1) [51, 52]; (ii) through an interaction with DCs [53]; and (iii) neutrophils are target cells for hMPV replication, thus the inhibition of viral load could be a consequential effect of a reduction of these innate immune cells.

Finally, no significant differences in lung gene expression of IL-4, IL-5, IL-10, IL-13, IFN-γ, and TNF-α were found in both experimental groups after 4 dpi. Nevertheless, an overall increase in IL-4, IL-5, and IL-10, but not IL-5, IL-13, and TNF-α occurred after 6 dpi in *tslpr*$^{-/-}$ mice. This was concomitant with a reduction of PMN cells within the airways. Thus, a lack of a functional TSLP-TSLPR pathway failed in supporting lung inflammation at later times pi. Taken together, TSLP could play a role in inducing the immunopathology caused by hMPV through the production of TARC/CCL17, IL5, IL-13, and TNF-α, in similar manner as previously reported upon activation of this pathway [19, 21, 25, 30, 42, 54]. These data strongly suggest an important contribution of the TSLP pathway in favoring hMPV inflammation and replication in the lung, either associated with or independent of the OX40L expression. Taken together, a proposed model shown in Figure 7 explains the mechanism behind the activation of the TSLP pathway by hMPV infection that results in excessive inflammation and viral replication. In summary, we have found that one of the main mechanisms causing lung inflammation and favoring viral replication in hMPV-infected mice is the TSLP pathway. Remarkably, we have also shown that by either genetically abrogating or immunologically blocking the TSLP-TSLPR pathway not only ameliorates significantly lung inflammation and damage but also reduces viral replication in hMPV-infected mice. This work makes a significant contribution to elucidating the hMPV immunopathology, an understanding of which could enable the development of new therapeutic treatments in preventing illness caused by hMPV infections. Our data support the notion that blocking of the TSLP pathway could be a potential therapy to reduce lung damage and viral replication upon hMPV infection.

Material and methods

Viruses and infection of AECs

LLC-MK2 cells (American Type Culture Collection) were used to propagate hMPV serogroup A, clinical isolate CZ0107 (clinical isolate obtained from the Laboratory of Infectology and Virology of the Clinical Hospital of the Pontificia Universidad Católica de Chile), and hRSV serogroup A2, strain 13018-8 (clinical isolate obtained from the Public Health Institute of Chile) [10, 55, 56]. Titration of hMPV and hRSV was performed over LLC-MK2 and HEp-2 monolayers as previously described [55, 56]. hMPV and hRSV inocula were routinely evaluated for LPS by using an endotoxin test and for species of *Mycoplasma* contamination by PCR.

Human alveolar type II like epithelial cells (A549 cells) (kindly provided by Dr. Pedro Piedra, Baylor College of Medicine, USA) were maintained in MEM medium containing 10% (v/v) FBS, 100 IU/mL penicillin, and 100 μg/mL streptomycin. A549 cells were inoculated either with mock (supernatant of uninfected LLC-MK2 cells), UV-inactivated hMPV or infectious hMPV at a MOI of either 0.1 or 1. Cell infection was performed by spinoculation at 700 × *g* for 1 h in OptiMem I Reduced Serum medium. Supernatants were removed and fresh medium was added to each well and incubated at 37°C in 5% CO_2 and harvested for viral RNA amplification analysis by qRT-PCR at 12, 24, and 48 h pi. Separately, A549 cells were infected with hRSV at a MOI of 1 for 24 h in a similar manner. Mock controls for hRSV-inoculated cells were obtained from uninfected HEp-2 cells. In addition, either 10 μg/mL LPS or 10 μg/mL polyI:C sodium were transfected into cells and used as controls for the induction of the different cytokines evaluated.

Infection of mice with hMPV

BALB/cJ mice were originally obtained from The Jackson Laboratory (Bar Harbor, ME, USA) and *tslpr*$^{-/-}$ mice were kindly provided by Dr. Warren Leonard [57], NIH (USA). All mice were maintained at the pathogen-free animal facility at the Pontificia Universidad Católica de Chile (Santiago, Chile). Mice (6–8 weeks old) were anesthetized with a mixture of ketamine (20 mg/kg)/xylazine (1 mg/kg) and inoculated by i.n. instillation of ~0.5–1 × 10^6 PFUs of hMPV or mock. Following infection, body weight was recorded daily for all groups. All animal work was performed according to institutional guidelines and supervised by a veterinarian.

Neutrophil depletion in mice

Six- to 8-week-old BALB/cJ WT mice and BALB/cJ *tslpr*$^{-/-}$ mice were depleted of neutrophils as previously reported [41]. Briefly, neutrophils were depleted with 1 mg of anti-Ly6G (1A8; Bio X Cell) given i.p. 2 days before infection. In addition, doses of 0.5 mg anti-Ly6G antibody were given to mice on days 0 and 2 pi. In addition, another group of mice were treated with rat IgG2a isotype control (2A3; Bio X Cell) on days –2 (1 mg), 0 (0.5 mg), and 2 (0.5 mg) by i.p. The results of these treatments are shown in Supporting Information Figure 7.

Flow cytometry analyses

At different days after infection, mice were terminally anesthetized by i.p. injection of a mixture of ketamine (110 mg/kg)/xylazine (5 mg/kg). BALF, lungs, previously perfused, lung draining MLN, and blood samples were collected as previously described [10] and analyzed by flow cytometry as shown in Supporting Information Figures 1–6. Briefly, lungs and MLN tissues were treated with 1 mg/mL collagenase type IV (Life Technologies). Samples were homogenized and filtered in cold PBS-10 mM EDTA using a 1-mL syringe plunger and a 40 μm cell strainer. Cellular suspensions were centrifuged at 300 × *g* for 5 min and pellets were washed, resuspended, and counted in a hematologic chamber or counted during flow cytometry acquisition using CountBright Absolute Counting Beads (Life Technologies). Cells were then stained with the following antibodies, according to each experiment: anti-CD11b-FITC (clone CBRM1.5) and anti-Gr-1-PE (Ly6G/Ly6C)-allophycocyanin (clone RB6-8C5) mAbs (BD Pharmingen); anti-Siglec-F-PE (clone E50-2440); anti-Ly-6G-PerCP Cy5.5 or -APC (clone 1A8); anti-CD11c- PE Cy7 (clone HL3); anti-I-A I-E-APC Cy7 (clone M5/114.15.2); anti-CD24-FITC (clone M1/69); anti-CD103- PerCP Cy5.5 (clone 2E7); anti-CD64-Alexa Fluor 488 (clone 290322); anti-PDCA-1-PE (clone 129C1); anti-CD56-PE (clone 809220); anti-CD49b-PE Cy7 (clone DX5); anti-TCRβ (clone H57), anti-CD4-PE Cy7 (clone GK1.5); anti-CD8a-APC Cy7 (clone 53–6.7); anti-CD11b-APC (clone M1/70); anti-CD24-PE (clone 30-F1); and anti–CD252 (OX40L)-APC or Alexa Fluor 647 (clone RM134L, Biolegend) mAbs.

For analysis of cytokine secretion by T cells, intracellular cytokines were measured as previously described [29]. Immediately after harvesting, lung cells were incubated in RPMI 1640 medium with 10 μg/mL Brefeldin A (premade solution from SIGMA-ALDRICH) for 5 h at 37°C and 5% CO_2. Then, cells were stained for 30 min at 4°C using a common T-cell panel, washed and fixed using 1% paraformaldehyde in PBS for 10 min at 4ºC, and finally permeabilized with 0.5% saponine, 0.5% BSA (in PBS), and stained ON at 4ºC with either anti-IFN-γ-PE (clone XMG1.2, BD Pharmingen), anti-IL-4-PE (clone 11B11, Biolegend), anti-IL-10-PE (clone JES5-16E3, Biolegend), anti-IL-12-PE (clone C15.6, BD Pharmingen), anti-IL-13-PE (clone eBio13A, ebioscience), or anti-TNF-α-PE (clone MP6-XT22). Data were acquired using the BD FACSDiva software and the FACSCanto II flow cytometer (BD Biosciences) and analyzed as shown in Supporting Information Figures 1–6, using FlowJo v X.0.7 (TreeStar Inc.) software.

Lung histopathology

Lungs removed from mice at different days pi were fixed in 4% paraformaldehyde and embedded in paraffin. For histopathology analysis, sections of 4 μm were obtained using a Thermo Scientific Microm HM 325 microtome and stained with H&E, as previously described [35]. The histopathological score was performed by a pathologist who also quantified the amount of PMN cells in the inflammatory infiltrates, involving peribronchial areas (peribronchiolitis) and interstitial/intra-alveolar zones (interstitial pneumonitis/alveolitis). Peribronchiolitis was assessed by counting the number of PMN cells per bronchiolar section in five high-power fields for each animal. Interstitial pneumonitis/alveolitis were determined in each animal by counting the total amount of PMN cells per high-power field, in a total of five images. Images and evaluation of the lung histological sections were obtained using an Olympus CKX41 inverted microscope and a Lumenera's Infinity 2 camera with the Infinity Analyze software.

Quantitative real-time PCR for cytokine expression

RNA from A549 cells exposed to the different treatments or from a lung section of mice was extracted using TRizol LS reagent (Invitrogen). Cytokine expression in cell lines or in murine lung samples was quantified by qRT-PCR from total RNA. Primers used to amply human RNA were as follows: TSLP, IL-33, and IL-8. Primers used to amplify murine RNA were as follows: TARC/CCL17, TSLP, IL-4, IL-5, IL-10, IL-13, IFN-γ, and TNF-α by means of the respective Taqman(R) Gene Expression assays (Applied Biosystems). Reactions from total RNA were performed using the TaqMan One-Step RT-PCR master mix reagent kit (Applied Biosystems) in a StepOne Plus thermocycler (Applied Biosystems), with the following cycling conditions: one cycle of 48°C for 15 min and 95°C for 10 min, followed by 40 cycles of 95°C for 15 s and 60°C for 1 min. Abundance of each target mRNA was determined by the relative quantification or comparative CT ($2^{-\Delta\Delta ct}$) method. Normalization versus endogenous control RNA was performed on samples using the TaqMan mouse beta (β)-actin or the Taqman human glyceraldehyde-3-phosphate dehydrogenase (GAPDH) control assays (Applied Biosystems). All samples were analyzed at least by triplicate.

Determination of viral RNA by qRT-PCR

Viral RNAs from cell cultures and lung tissues were determined similarly, as previously described [10]. Briefly, total RNA was isolated using TRIzol LS reagent (Life Technologies) and 1 μg RNA was reverse transcribed to cDNA using the ImProm-II reverse transcription system kit (Promega, Madison, WI, USA), according to manufacturer's instructions. The hMPV-N gene was amplified by qRT-PCR using the following primers: 5′-ACAGCAGATTCTAAGAAACTCAGG-3′ (forward) and 5′-TCTTTGTCTATCTCTTCCACCC-3′ (reverse) with an amplicon length of 153 bp, as previously described [10, 56]. Mouse β-actin, a housekeeping reference gene, was also amplified using the primers 5′-AGGCAT CCTGACCCTGAAGTAC-3′ (forward) and 5′-TCTTCATGAGGTAGTCTGTCAG-3′ (reverse) with an amplicon length of 384 bp. qPCR reactions were performed using the Fast qPCR Master Mix (Applied Biosystem) in a StepOne Plus thermocycler (Applied Biosystems). Standard curves for absolute quantification were generated from increasing concentrations

of the templates N-hMPV and β-actin plasmids. Standard curves included five tenfold dilutions and three replicate wells for each dilution.

Statistical analyses

When indicated, p values were calculated using the GraphPad Prism software v5 (GraphPad Software, Inc.). As indicated in figure legends, several statistical analyses, including unpaired Student's t-test, Mann–Whitney U-test, one-way ANOVA, or two-way ANOVA, were used to calculate statistical significance. p values of < 0.05 were considered to be significant.

Acknowledgments: We thank Dr. Leonard Warren (NIH, USA) for providing us the *tslpr*$^{-/-}$ mice. We also thank Dr. Pedro Piedra (Baylor College of Medicine, USA) for kindly providing us the A549 cells. We also thank Dr. KJ Sastry (The University of Texas M. D. Anderson Cancer Center, USA) for providing us protocols and valuable scientific discussion. We thank Maria Olga Bargsted D.V.M. and Alfredo Bermudez D.V.M. (PUC, Chile) for maintaining the mouse colonies that were used in this work as well in helping us in animal management. We also thank Geraldyne Salazar and Nicolás Gálvez for technical support. Authors are supported by grant numbers 3120019, 3140455, 1070352, 1050979, 1040349, 1100926, 1110397, 1100971 and 1110604 from the National Fund for Scientific and Technological Development (FONDECYT) program of the ministry of Education of Chile; and by grant P09-016-F from the Millennium Institute in Immunology and Immunotherapy of the ministry of Economy of Chile. AMK is a Chaire De La Région Pays De La Loire De Chercheur Étranger D'excellence.

Conflict of interest: The authors declare no financial or commercial conflict of interest.

References

1 **Van den Hoogen, B. G., Bestebroer, T. M., Osterhaus, A. D. M. E. and Fouchier, R. A. M.** Analysis of the genomic sequence of a human metapneumovirus. *Virology* 2002. **295**: 119–132.

2 **Bastien, N., Normand, S., Taylor, T., Ward, D., Peret, T. C., Boivin, G., Anderson, L. J. et al.**, Sequence analysis of the N, P, M and F genes of Canadian human metapneumovirus strains. *Virus Res.* 2003. **93**: 51–62.

3 **Van den Hoogen, B. G., de Jong, J. C., Groen, J., Kuiken, T., de Groot, R., Fouchier, R. A., Osterhaus, A. D.** A newly discovered human pneumovirus isolated from young children with respiratory tract disease. *Nat Med.* 2001. **7**: 719–724.

4 **Kahn, J. S.** Epidemiology of human metapneumovirus. *Clin Microbiol. Rev.* 2006. **19**: 546–557.

5 **Boivin, G., De Serres, G., Côté, S., Gilca, R., Abed, Y., Rochette, L., Bergeron, M. G. et al.**, Human metapneumovirus infections in hospitalized children. *Emerg. Infect. Dis.* 2003. **9**: 634–640.

6 **Caracciolo, S., Minini, C., Colombrita, D., Rossi, D., Miglietti, N., Vettore, E., Caruso, A. et al.**, Human metapneumovirus infection in young children hospitalized with acute respiratory tract disease: virologic and clinical features. *Pediatr. Infect. Dis. J.* 2008. **27**: 406–412.

7 **Freymouth, F., Vabret, A., Legrand, L., Eterradossi, N., Lafay-Delaire, F., Brouard, J. and Guillois B.** Presence of the new human metapneumovirus in French children with bronchiolitis. *Pediatr. Infect. Dis. J.* 2003. **22**: 92–94.

8 **Feuillet, F., Lina, B., Rosa-Calatrava, M. and Boivin, G.** Ten years of human metapneumovirus research. *J. Clin. Virol.* 2012. **53**: 97–105.

9 **Boivin, G., De Serres, G., Hamelin, M.-E., Côté, S., Argouin, M., Tremblay, G., Maranda-Aubut, R. et al.**, An outbreak of severe respiratory tract infection due to human metapneumovirus in a long-term care facility. **2007**. 1152–1158.

10 **Palavecino, C. E., Cespedes, P. F., Gomez, R. S., Kalergis, A. M. and Bueno, S. M.** Immunization with a recombinant Bacillus Calmette-Guerin strain confers protective Th1 immunity against the human metapneumovirus. *J. Immunol.* 2014. **192**: 214–223.

11 **Biacchesi, S., Skiadopoulos, M. H., Yang, L., Lamirande, E. W., Tran, K. C., Murphy, B. R., Collins, P. L. et al.**, Recombinant human Metapneumovirus lacking the small hydrophobic SH and/or attachment G glycoprotein: deletion of G yields a promising vaccine candidate. *J. Virol.* 2004. **78**: 12877–12887.

12 **Liu, P., Shu, Z., Qin, X., Dou, Y., Zhao, Y. and Zhao, X.** A live attenuated human metapneumovirus vaccine strain provides complete protection against homologous viral infection and cross-protection against heterologous viral infection in BALB/c mice. *Clin. Vaccine Immunol.* 2013. **20**: 1246–1254.

13 **Alvarez, R. and Tripp, R. A.** The immune response to human metapneumovirus is associated with aberrant immunity and impaired virus clearance in BALB/c mice. *J. Virol.* 2005. **79**: 5971–5978.

14 **Hamelin, M-E, Prince, G. A., Gomez, A. M., Kinkead, R. and Boivin, G.** Human metapneumovirus infection induces long-term pulmonary inflammation associated with airway obstruction and hyperresponsiveness in mice. *J. Infect. Dis.* 2006. **193**: 1634–1642.

15 **Kuiken, T., van den Hoogen, B. G., van Riel, D. A., Laman, J. D., van Amerongen, G., Sprong, L., Fouchier, R. A. et al.**, Experimental human metapneumovirus infection of cynomolgus macaques (Macaca fascicularis) results in virus replication in ciliated epithelial cells and pneumocytes with associated lesions throughout the respiratory tract. *Am. J. Pathol.* 2004. **164**: 1893–1900.

16 **Esper, F., Boucher, D., Weibel, C., Martinello, R. A. and Kahn, J. S.** Human metapneumovirus infection in the United States: clinical manifestations associated with a newly emerging respiratory infection in children. *Pediatrics* 2003. **111**: 1407–1410.

17 **Huck, B., Neumann-Haefelin, D., Schmitt-Graeff, A., Weckmann, M., Mattes, J., Ehl, S. and Falcone, V.** Human metapneumovirus induces more severe disease and stronger innate immune response in BALB/c mice as compared with respiratory syncytial virus. *Respir. Res.* 2007. **8**: 6.

18 **Guerrero-Plata, A., Casola, A. and Garofalo R. P.** Human metapneumovirus induces a profile of lung cytokines distinct from that of respiratory syncytial virus. *J. Virol.* 2005. **79**: 14992–14997.

19 **Kolli, D., Bataki, E. L., Spetch, L., Guerrero-Plata, A., Jewell, A. M., Piedra, P. A., Milligan, G. N. et al.**, T lymphocytes contribute to antiviral immunity and pathogenesis in experimental human metapneumovirus infection. *J. Virol.* 2008. **82**: 8560–8569.

20 **Fietta, P. and Delsante, G.** The effector T helper cell triade. *Riv. Biol.* 2009. **102**: 61–74.

21 **Romagnani, S.** Regulation of the T cell response. *Clin. Exp. Allergy*. 2006. **36**: 1357–1366.

22 **Liu, Y. J.** Thymic stromal lymphopoietin: master switch for allergic inflammation. *J. Exp. Med*. 2006. **203**: 269–273.

23 **Ziegler, S. F. and Liu, Y. J.** Thymic stromal lymphopoietin in normal and pathogenic T cell development and function. *Nat. Immunol*. 2006. **7**: 709–714.

24 **Soumelis, V., Reche, P. A., Kanzler, H., Yuan, W., Edward, G., Homey, B., Gilliet, M. et al.**, Human epithelial cells trigger dendritic cell mediated allergic inflammation by producing TSLP. *Nat. Immunol.* 2002. **3**: 673–680.

25 **Ying, S., O'Connor, B., Ratoff, J., Meng, Q., Mallett, K., Cousins, D., Robinson, D. et al.**, Thymic stromal lymphopoietin expression is increased in asthmatic airways and correlates with expression of Th2-attracting chemokines and disease severity. *J. Immunol*. 2005. **174**: 8183–8190.

26 **Yoo, J., Omori, M., Gyarmati, D., Zhou, B., Aye, T., Brewer, A., Comeau, M. R. et al.**, Spontaneous atopic dermatitis in mice expressing an inducible thymic stromal lymphopoietin transgene specifically in the skin. *J. Exp. Med*. 2005. **202**: 541–549.

27 **Zhou, B., Comeau, M. R., De Smedt, T., Liggitt, H. D., Dahl, M. E., Lewis, D. B., Gyarmati, D. et al.**, Thymic stromal lymphopoietin as a key initiator of allergic airway inflammation in mice. *Nat. Immunol*. 2005. **6**: 1047–1053.

28 **Li, Y. L., Li, H. J., Ji, F., Zhang, X., Wang, R., Hao, J. Q., Bi, W. X. et al.**, Thymic stromal lymphopoietin promotes lung inflammation through activation of dendritic cells. *J. Asthma*. 2010. **47**: 117–123.

29 **Arestides, R. S., He, H., Westlake, R. M., Chen, A. I., Sharpe, A. H., Perkins, D. L. and Finn, P. W.** Costimulatory molecule OX40L is critical for both Th1 and Th2 responses in allergic inflammation. *Eur. J. Immunol*. 2002. **32**: 2874–2880.

30 **Dannull, J., Nair, S., Su, Z., Boczkowski, D., DeBeck, C., Yang, B., Gilboa, E. et al.**, Enhancing the immunostimulatory function of dendritic cells by transfection with mRNA encoding OX40 ligand. *Blood* 2005. **105**: 3206–3213.

31 **Ito, T., Wang, Y. H., Duramad, O., Hori, T., Delespesse, G. J., Watanabe, N., Qin, F. X. et al.**, TSLP-activated dendritic cells induce an inflammatory T helper type 2 cell response through OX40 ligand. *J. Exp. Med*. 2005. **202**: 1213–1223.

32 **Liu, Y. J.**, Thymic stromal lymphopoietin and OX40 ligand pathway in the initiation of dendritic cell-mediated allergic inflammation. *J. Allergy Clin. Immunol*. 2007. **120**: 236–238.

33 **Qiao, J., Li, A. and Jin, X.** TSLP from RSV-stimulated rat airway epithelial cells activates myeloid dendritic cells. *Immunol. Cell Biol*. 2011. **89**: 231–238.

34 **Lee, H. C., Headley, M. B., Loo, Y. M., Berlin, A., Gale, M., Jr., Debley, J. S., Lukacs, N. W. et al.**, Thymic stromal lymphopoietin is induced by respiratory syncytial virus-infected airway epithelial cells and promotes a type 2 response to infection. *J. Allergy Clin. Immunol*. 2012. **130**: 1187–1196. e5.

35 **Han, J., Dakhama, A., Jia, Y., Wang, M., Zeng, W., Takeda, K., Shiraishi, Y. et al.**, Responsiveness to respiratory syncytial virus in neonates is mediated through thymic stromal lymphopoietin and OX40 ligand. *J. Allergy Clin. Immunol*. 2012. **130**: 1175–1186. e9.

36 **Ueta, M., Mizushima, K., Yokoi, N., Naito, Y. and Kinoshita, S.** Gene-expression analysis of polyI:C-stimulated primary human conjunctival epithelial cells. *Br. J. Ophthalmol*. 2010. **94**: 1528–1532.

37 **Yagami, A., Orihara, K., Morita, H., Futamura, K., Hashimoto, N., Matsumoto, K., Saito, H. et al.**, IL-33 mediates inflammatory responses in human lung tissue cells. *J. Immunol*. 2010. **185**: 5743–5750.

38 **Besnard, A. G., Togbe, D., Guillou, N., Erard, F., Quesniaux, V. and Ryffel, B.** IL-33-activated dendritic cells are critical for allergic airway inflammation. *Eur. J. Immunol*. 2011. **41**: 1675–1686.

39 **Misharin, A. V., Morales-Nebreda, L., Mutlu, G. M., Budinger, G. R. S. and Perlman, H.** Flow cytometric analysis of macrophages and dendritic cell subsets in the mouse lung. *Am. J. Respir. Cell Mol. Biol*. 2013. **49**: 503–510.

40 **Besnard, A. G., Togbe, D., Guillou, N., Erard, F., Quesniaux, V. and Ryffel, B.** IL-33-activated dendritic cells are critical for allergic airway inflammation. *Eur. J. Immunol*. 2011. **41**: 1675–1686.

41 **Stokes, K. L., Currier, M. G., Sakamoto, K., Lee, S., Collins, P. L., Plemper, R. K. and Moore, M. L.** The respiratory syncytial virus fusion protein and neutrophils mediate the airway mucin response to pathogenic respiratory syncytial virus infection. *J. Virol*. 2013. **87**: 10070–10082.

42 **Xing, Z., Jordana, M., Kirpalani, H., Driscoll, K. E., Schall, T. J. and Gauldie, J.** Cytokine expression by neutrophils and macrophages in vivo: endotoxin induces tumor necrosis factor-alpha, macrophage inflammatory protein-2, interleukin-1 beta, and interleukin-6 but not RANTES or transforming growth factor-beta 1 mRNA expression in acut. *Am. J. Respir. Cell Mol. Biol*. 1994. **10**: 148–153.

43 **Krause, P., Bruckner, M., Uermösi, C., Singer, E., Groettrup, M. and Legler, D. F.** Prostaglandin e2 enhances T-cell proliferation by inducing the costimulatory molecules OX40L, CD70, and 4-1BBL on dendritic cells. *Blood* 2009. **113**: 2451–2460.

44 **Beck-Schimmer, B., Schwendener, R., Pasch, T., Reyes, L., Booy, C. and Schimmer, R. C.** Alveolar macrophages regulate neutrophil recruitment in endotoxin-induced lung injury. *Respir. Res*. 2005. **6**: 61.

45 **Ito, T., Amakawa, R., Inaba, M., Hori, T., Ota, M., Nakamura, K., Takebayashi, M. et al.**, Plasmacytoid dendritic cells regulate Th cell responses through OX40 ligand and type I IFNs. *J. Immunol*. 2004. **172**: 4253–4259.

46 **Inngjerdingen, M., Damaj, B. and Maghazachi, A. A.** Human NK cells express CC chemokine receptors 4 and 8 and respond to thymus and activation-regulated chemokine, macrophage-derived chemokine, and I-309. *J. Immunol*. 2000. **164**: 4048–4054.

47 **Warren, H. S., Kinnear, B. F., Phillips, J. H. and Lanier, L. L.** Production of IL-5 by human NK cells and regulation of IL-5 secretion by IL-4, IL-10, and IL-12. *J. Immunol*. 1995. **154**: 5144–5152.

48 **Korsgren, M., Persson, C. G., Sundler, F., Bjerke, T., Hansson, T., Chambers, B. J., Hong, S. et al.**, Natural killer cells determine development of allergen-induced eosinophilic airway inflammation in mice. *J. Exp. Med*. 1999. **189**: 553–562.

49 **Lee, H. C., Headley, M. B., Loo, Y. M., Berlin, A., Gale, Jr. M, Debley, J. S., Lukacs, N. W. et al.**, Thymic stromal lymphopoietin is induced by respiratory syncytial virus-infected airway epithelial cells and promotes a type 2 response to infection. *J. Allergy Clin. Immunol*. 2012. **130**: 1187–1196. e5.

50 **Chambers, B. J., Salcedo, M. and Ljunggren, H. G.** Triggering of natural killer cells by the costimulatory molecule CD80 (B7-1). *Immunity* 1996. **5**: 311–317.

51 **Schmielau, J. and Finn, O. J.** Activated granulocytes and granulocyte-derived hydrogen peroxide are the underlying mechanism of suppression of t-cell function in advanced cancer patients. *Cancer Res*. 2001. **61**: 4756–4760.

52 **Sippel, T. R., White, J., Nag, K., Tsvankin, V., Klaassen, M., Kleinschmidt-DeMasters, B. K. and Waziri, A.** Neutrophil degranulation and immunosuppression in patients with GBM: restoration of cellular immune function by targeting arginase I. *Clin. Cancer Res*. 2011. **17**: 6992–7002.

53 **Doz, E., Lombard, R., Carreras, F., Buzoni-Gatel, D. and Winter, N.** Mycobacteria-infected dendritic cells attract neutrophils that produce IL-10 and specifically shut down Th17 CD4 T cells through their IL-10 receptor. *J. Immunol.* 2013. **191**: 3818–3826.

54 **Arestides, R. S., He, H., Westlake, R. M., Chen, A. I., Sharpe, A. H., Perkins, D. L. and Finn, P. W.** Costimulatory molecule OX40L is critical for both Th1 and Th2 responses in allergic inflammation. *Eur. J. Immunol.* 2002. **32**: 2874–2880.

55 **Bueno, S. M., Gonzalez, P. A., Cautivo, K. M., Mora, J. E., Leiva, E. D., Tobar, H. E., Fennelly, G. J. et al.**, Protective T cell immunity against respiratory syncytial virus is efficiently induced by recombinant BCG. *Proc. Natl. Acad. Sci. USA* 2008. **105**: 20822–20827.

56 **Cespedes, P. F., Gonzalez, P. A. and Kalergis, A. M.** Human metapneumovirus keeps dendritic cells from priming antigen-specific naive T cells. *Immunology* 2013. **139**: 366–376.

57 **Al-Shami, A., Spolski, R., Kelly, J., Fry, T., Schwartzberg, P. L., Pandey, A., Mackall, C. L. et al.**, A role for thymic stromal lymphopoietin in CD4(+) T cell development. *J. Exp. Med.* 2004. **200**: 159–168.

Abbreviations: **AEC**: airway epithelial cell · **dpi**: days postinfection · **hMPV**: human metapneumovirus · **hRSV**: human respiratory syncytial virus · **N**: nucleoprotein · **OX40L**: OX40 ligand · **pi**: postinfection · **qRT**: quantitative reverse transcriptase · **TARC**: thymus and activation-regulated chemokine · **TSLP**: thymic stromal lymphopoietin · ***tslpr*$^{-/-}$**: TSLP receptor deficient mice

Full correspondence: Dr. Alexis M. Kalergis, Departamento de Genética Molecular y Microbiología, Facultad de Ciencias Biológicas, Millennium Institute on Immunology and Immunotherapy, Pontificia Universidad Católica de Chile. Alameda 340, Santiago E-8331010, Chile
Fax: +56-2-222-5515
e-mail: akalergis@bio.puc.cl

Received: 10/7/2014
Revised: 28/1/2015
Accepted: 10/3/2015
Accepted article online: 12/3/2015

